Infrared detectors for wavefront sensing

Jean-Luc Gach[a,b,*], Philippe Feautrier[a,c], Eric Stadler[a,c], Fabien Clop[a], Stephane Lemarchand[a], Thomas Carmignani[a], Yann Wanwanscappel[a], Carine Doucure[a,] David Boutolleau[a]

[a]First Light Imaging S.A.S. 100, Route des houillères, 13590 Meyreuil, France;
[b] Aix Marseille Université, CNRS, LAM (Laboratoire d'Astrophysique de Marseille) UMR 7326, 13388 Marseille, France;
[c] Univ. Grenoble Alpes, CNRS, IPAG, F-38000 Grenoble, France ;

*jeanluc.gach@first-light.fr; phone +33 442612920, www.firstlight.fr

ABSTRACT

After the development of the OCAM2 EMCCD fast visible camera [1] dedicated to advanced adaptive optics wavefront sensing, First Light Imaging moved to the SWIR fast cameras with the development of the C-RED One and the C-RED 2 cameras.

First Light Imaging's C-RED One infrared camera is capable of capturing up to 3500 full frames per second with a subelectron readout noise and very low background. C-RED One is based on the last version of the SAPHIRA detector developed by Leonardo UK. This breakthrough has been made possible thanks to the use of an e-APD infrared focal plane array which is a real disruptive technology in imagery. C-RED One is an autonomous system with an integrated cooling system and a vacuum regeneration system. It operates its sensor with a wide variety of read out techniques and processes video on-board thanks to an FPGA. We will show its performances and expose its main features.

In addition to this project, First Light Imaging developed an InGaAs 640x512 fast camera with unprecedented performances in terms of noise, dark and readout speed based on the SNAKE SWIR detector from Sofradir. The camera was called C-RED 2. The C-RED 2 characteristics and performances will be described.

The project leading to this application has received funding from the European Union's Horizon 2020 research and innovation program under grant agreement N° 673944. C-RED2 development is supported by the "Investments for the future" program and the Provence Alpes Côte d'Azur Region, in the frame of the CPER.

Keywords: infrared camera, e-apd, high speed, low noise, InGaAs, SWIR, 640 x 512 InGaAs.

1. INTRODUCTION

The Saphira Detector and C-RED One camera

Designed and fabricated by Leonardo UK, formerly Selex, the Saphira detector is designed for high speed infrared applications and is the result of a development program alongside the European Southern Observatory on sensors for astronomical instruments [2], [3], [4]. It delivers world leading photon sensitivity of <1 photon rms with Fowler sampling and high speed non-destructive readout (>10K frame/s). Saphira is an HgCdTe avalanche photodiode (APD) array incorporating a full custom ROIC for applications in the 1 to 2.5µm range. C-RED One camera is an autonomous plug-and-play system with a user-friendly interface, which can be operated in extreme and remote locations. The sensor is placed in a sealed vacuum environment and cooled down to cryogenic temperature using an integrated pulse tube. The vacuum is self-managed by the camera and no human intervention is required. The system shown in Figure 1 has been extensively described by Feautrier et al. in 2017 [5].

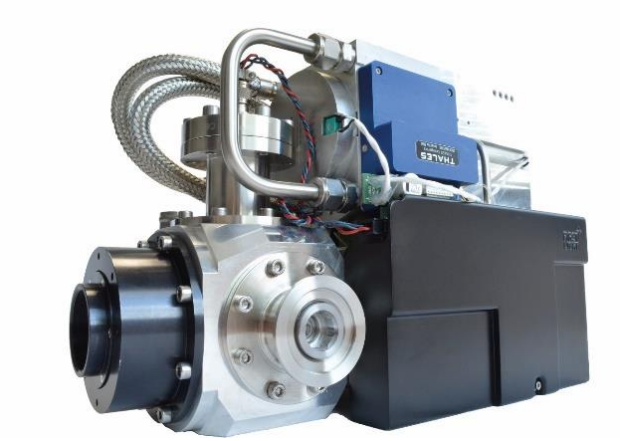

Figure 1: C-RED One camera. The cooling system (pulse tube) can be seen on the top whereas in the bottom are the vacuum cryostat and the readout electronics.

2. MEASURED C-RED ONE PERFORMANCES

The measurements were all made at 80K operating temperature, using a MARK 13 engineering grade SAPHIRA device. This device is supposed working as a science grade except for cosmetics which should be degraded.

Quantum efficiency

The array quantum efficiency peaks up to near 80% and the array AR coating may be optimized for J, H or K bands (H band is the standard one). Figure 2 shows the effect of this QE optimization. Moreover due to junction heterostructure with 3.5µm cutoff wavelength HgCdTe material for the avalanche multiplication region and 2.5 µm material for the absorber, the device is sensitive in L band at gain 1 but not with APD gain. This is due to photon penetration depth (longer wavelength photons penetrate deeper in the material and therefore are less amplified). We've measured that already with low gains (in the range of 5 to 10) the L band sensitivity is decreased to near zero, leaving only J, H and K sensitivity.

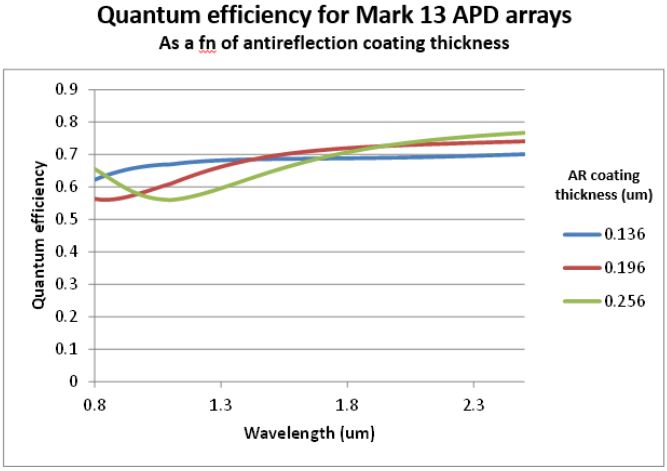

Figure 2: AR coating and QE optimization for J, H or K bands of Mark13 e-APD diodes. The H band coating is the standard one.

System gain

The system gain is measured illuminating the sensor with a flat field through an integrating sphere. Then temporal noise versus illumination level is plotted in log/log scale to have the system gain and the noise level (see Figure 3). The system

gain in an infrared device depends strongly upon the diode polarization. Indeed the diode capacitance is used to integrate the charges and its value depends on the reverse voltage applied (the higher, the lower is the diode capacitance). For a 2V reverse bias, which corresponds to a gain of 1, the system gain was measured at 1.1e^-/ADU which is in perfect accordance with the expected 1.15 e^-/ADUsystem gain with a 28fF node capacitance.

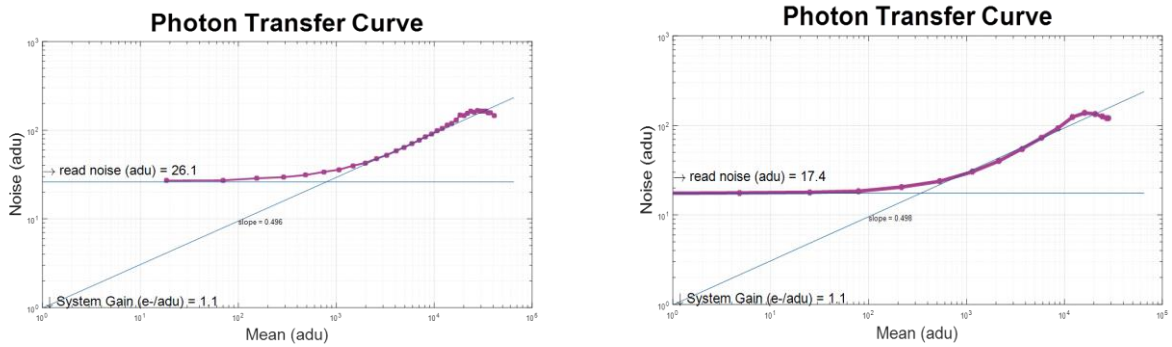

Figure 3: Photon transfer curve of single readout mode (left) and CDS mode (right).

APD gain

APD gain is measured by illuminating the sensor with a weak laser light at 1300nm. APD gain is then applied, and the ratio of ADU change over reference level gives the gain. To get rid from any FPN, the level measurement is done computing the electron flow in multiple non-destructive mode. Figure 4 shows that APD gain vs bias voltage and the exponential fit. The gain can be expressed as $G=0.309e^{0.395Vbias}$ which is in accordance with other measurements carried out by various groups using these devices.

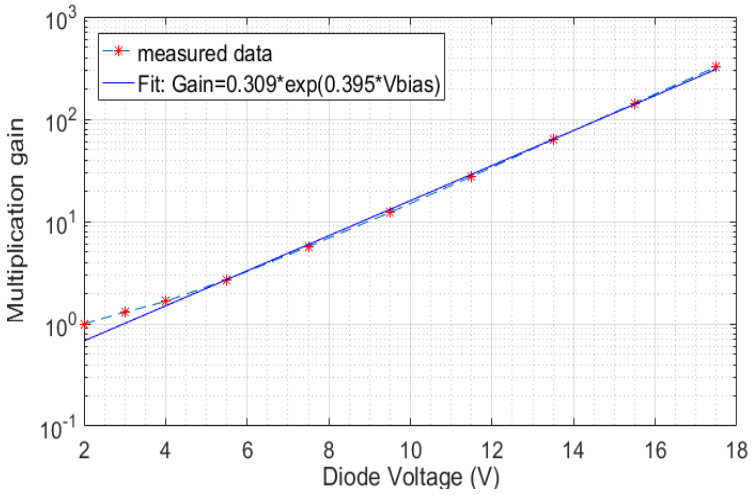

Figure 4: Measured APD gain vs polarization voltage of MARK 13 array and exponential fit.

System noise

The noise measurement is done by measuring the temporal variation of the image, sensor in the dark running at 1700fps.

Taking into account 28fF node capacitance, the KTC noise should be in the range of 35e- at 80K. Figure 5 shows the sensor readout noise in single readout and CDS readout modes. It can be noticed that the CDS mode reduces the readout noise by the KTC noise at the expense of a supplementary readout, hence a reduction in the maximal frame rate by a factor of two. It might be noticed that the noise scales perfectly with APD gain, therefore increasing APD gain does not increase

readout noise as it should be expected. Finally it can be noticed also that for gains > 30, the array enters in subelectron readout whatever is the readout mode (single readout or CDS). This is really a change of paradigm in the way of operating infrared arrays since CDS is no more needed to minimize readout noise, simply by increasing the APD gain, one can have very low noise operation, without compromise on readout speed, but at the expanse of a lower dynamic range (typically 30% less dynamic range in our case).

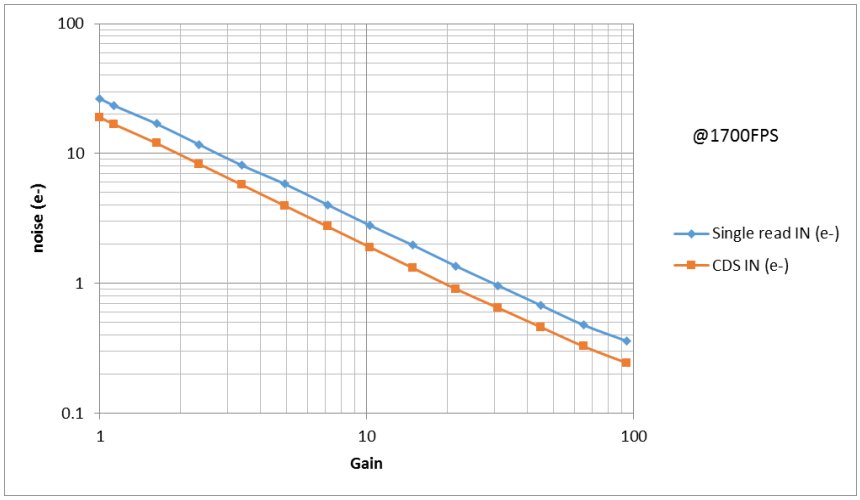

Figure 5: Measured input referred readout noise vs APD gain for single readout and CDS readout.

Dark current

To do this measurement the sensor is in the dark, looking at a 80K cold stop. The dark current is measured by fitting a line over the ADU level vs exposure time graph. The slope of this line gives the mean dark count. The measurements show that the dark current depends on the readout mode and the readout speed of the sensor as plotted in Figure 6. This is due to ROIC glowing.

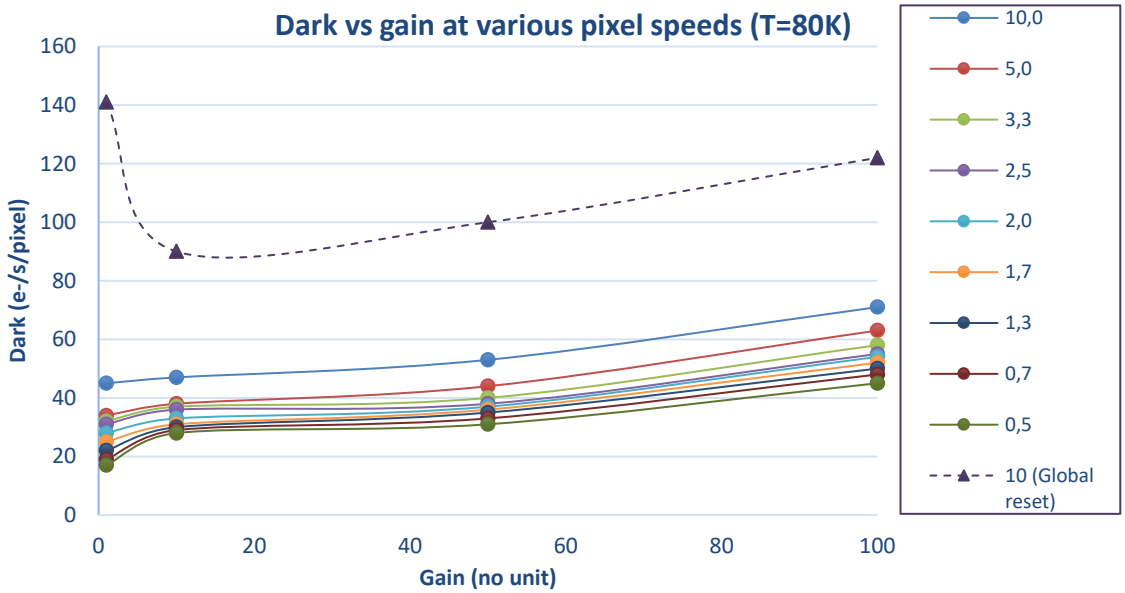

Figure 6: Measured dark current vs gain at different speed (right scale in MHz) and readout modes

Background measurement

The background current is measured the same way it is for the dark current but looking at a room temperature blackbody.

The operation is repeated for several gains. The result is plotted in Figure 7. The dark is increased for low and high gains. At low gains the sensor is sensitive up to 3.5 um, therefore more sensitive to photon leakage, whereas at high gains the dark current should be limited by trap assisted tunneling.

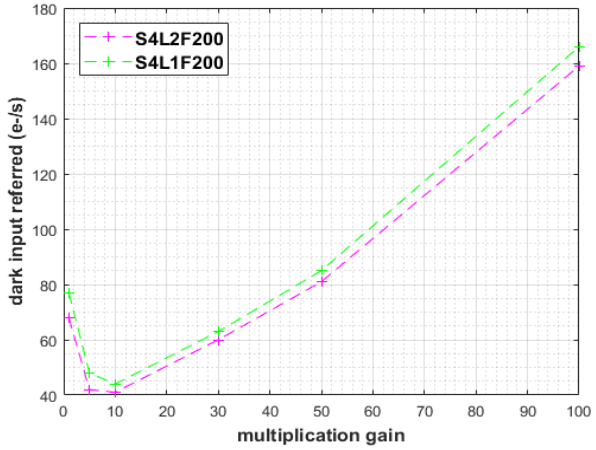

Figure 7: Background measurement vs gain at 400 FPS (purple) and 800 FPS (green)

Cosmetics

One of the advantage of this sensor is its extremely good cosmetics, even when high gain is applied. Some other groups reported only a few dead pixels over the entire array, which is due to the HgCdTe growing process (MOVPE). Even with our engineering grade device, the cosmetics was excellent only showing a few pixels with leakage dark current (See Figure 8). Shows images at various gains. e-APDs are not sensitive to overillumination.

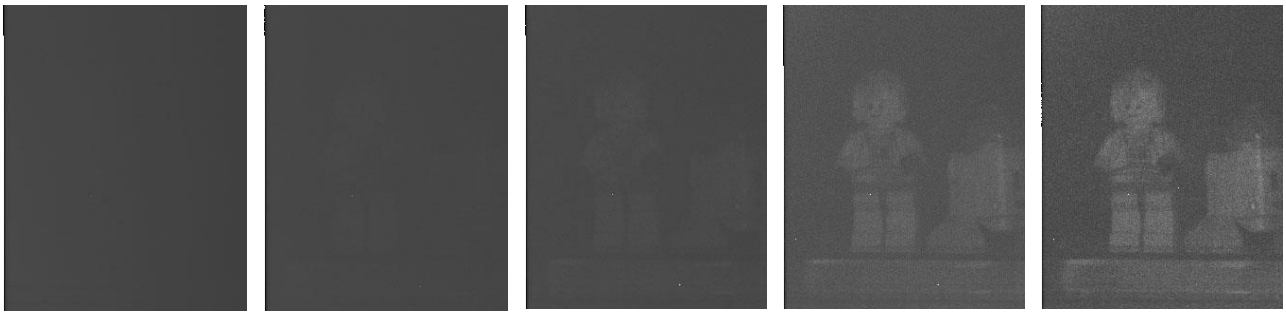

Figure 8: Low light scene imaged with gains of 1,6,13,45 and 90 (from left to right) showing only a few defective pixels at high gain (<10 defective pixels) on our engineering grade device, CDS readout at 1700 FPS.

On-Board Bias Processing

C-RED One can compute by itself a bias image by meaning 1000 successive frames. This operation is done by the embedded firmware. Each frame outputs by the camera is then be subtracted on-the-fly by this bias image. It is also possible to send a custom bias to the camera or get the one computed on-board. The system is also capable of doing a flat (NUC) correction on the same basis. Figure 9 shows the example of bias correction.

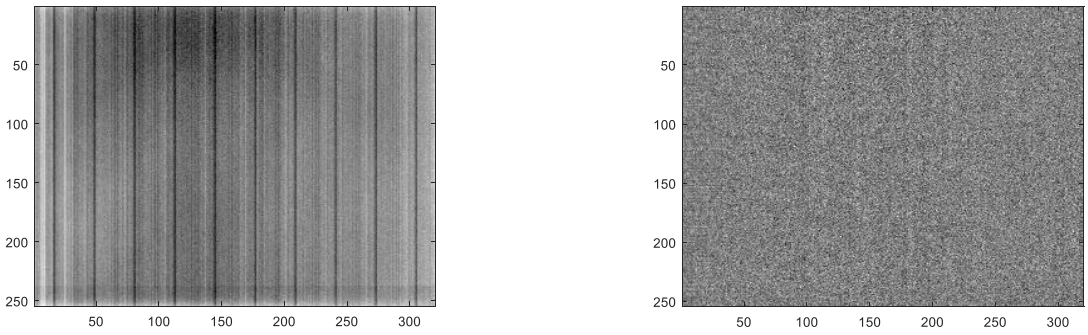

Figure 9: Example of Bias Processing. Left: Raw Image. Right : Bias processed Image.

Multiple Non-Destructive Reads.

C-RED One can operate the sensor in multiple non-destructives reads mode. This mode permits to reset the focal plane once and then read a burst of frames (see Figure 10).

Figure 10: Bursts of multiple non-destructive reads.

The level will increase as electrons are accumulating in the integration capacitance. The slope will then provide information of flux as highlighted in Figure 11).

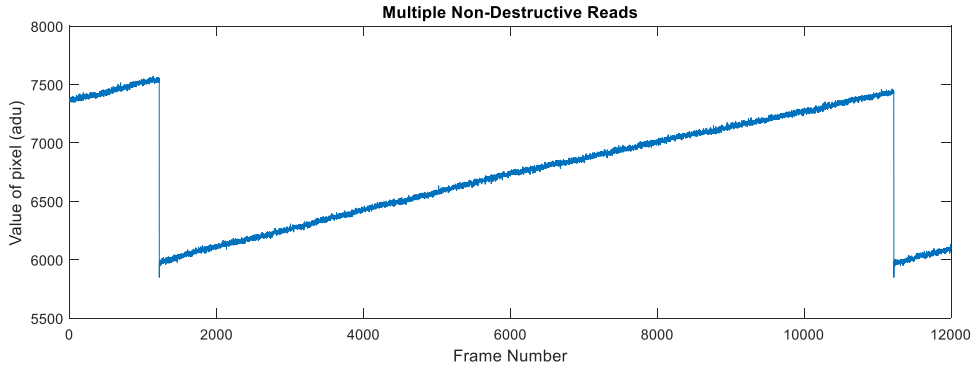

Figure 11: 10 000 successive reads in Global Shutter mode. Hot subject seen through K and H filters at gain 1.

Bias Drift.

The mean level of some pixels is plot during 33 hours with a tick of 1s. C-RED One runs in Global Shutter mode with correlated double sampling at full speed.

Every mean level is processed with 100 samples to reduce the noise.

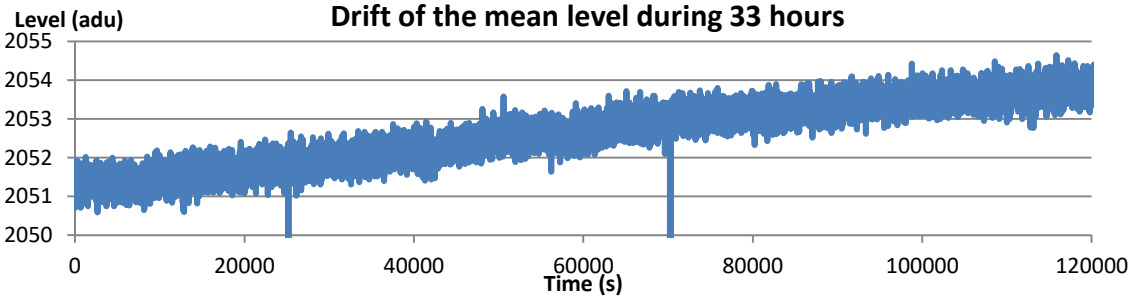

Figure 12: Bias drift measurement over 33 hours.

Finally, the drift of C-RED One is as low as 0.1adu/h and shown in Figure 12.

3. THE C-RED 2 640X512 InGaAs SWIR camera from First Light Imaging

C-RED 2 is a high performance, high speed low noise camera designed for Short Wave InfraRed imaging based on the SNAKE detector from Sofradir [6], [7], [8], [9]. Thanks to its state of the art electronics, software, and innovative mechanics, C-RED 2 is capable of unprecedented performances: up to 400 images per second with a read out noise from 10 to 30 electrons. To achieve these performances, C-RED 2 integrates a 640 x 512 InGaAs PIN Photodiode detector with 15 µm pixel pitch for high resolution, which embeds an electronic shutter with integration pulses shorter than 10 µs. C-RED 2 is also capable of windowing and multiple regions of interest (ROI), allowing faster image rate while maintaining a very low noise.

The software allows real time applications, and the interface is CameraLink full and superspeed USB3. C-RED 2 is designed to be updated remotely, and needs no human assistance to manage the cooling. The camera can operate in very low-light conditions as well as remote locations. Designed for high-end SWIR applications, smart and compact (see Figure 13), C-RED 2 is operating from 0.9 to 1.7 µm with a very good Quantum Efficiency over 70%, offering new opportunities for industrial or scientific applications.

Figure 13: Picture of the C-RED2 camera

The Table 1 summarizes the main features and preliminary performances of the CRED-2 camera.

C-RED 2 PERFORMANCES

Test measurement	Result	Unit
Maximum speed	400	FPS
Mean Dark + Readout Noise at 400 fps	30	e-
Quantization	14	bit
Detector Operating Temperature	-40	C°
Flat Quantum Efficiency from 0.9 to 1.7 µm	>70	%
Operability	99.7	%
Image Full well capacity at low gain, 400 fps	1400	ke-
Image Full well capacity at high gain, 400 fps	43	ke-

Table 1: typical performances and main features of the CRED-2 640x512 InGaAs SWIR camera.

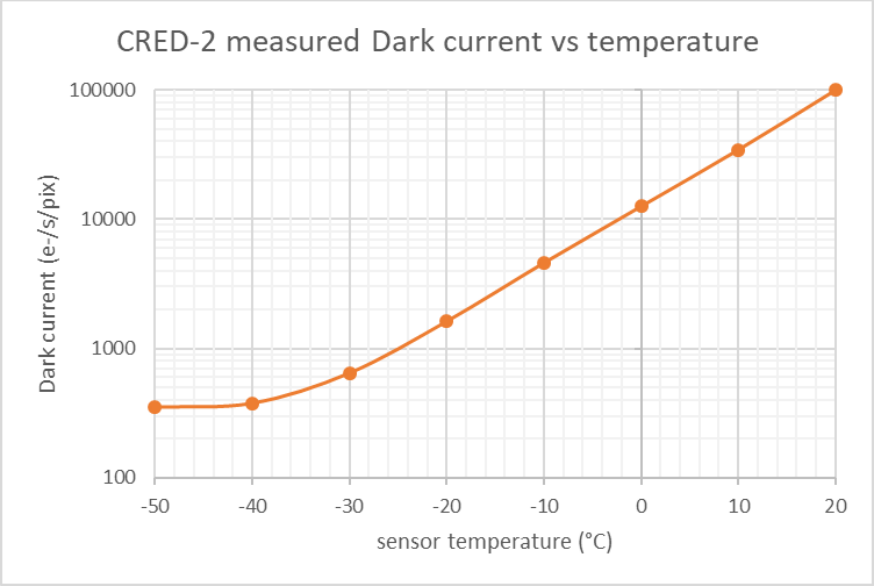

Figure 14 : C-RED 2 typical Dark (in e/s/pixel) as a function of the temperature (in °C).

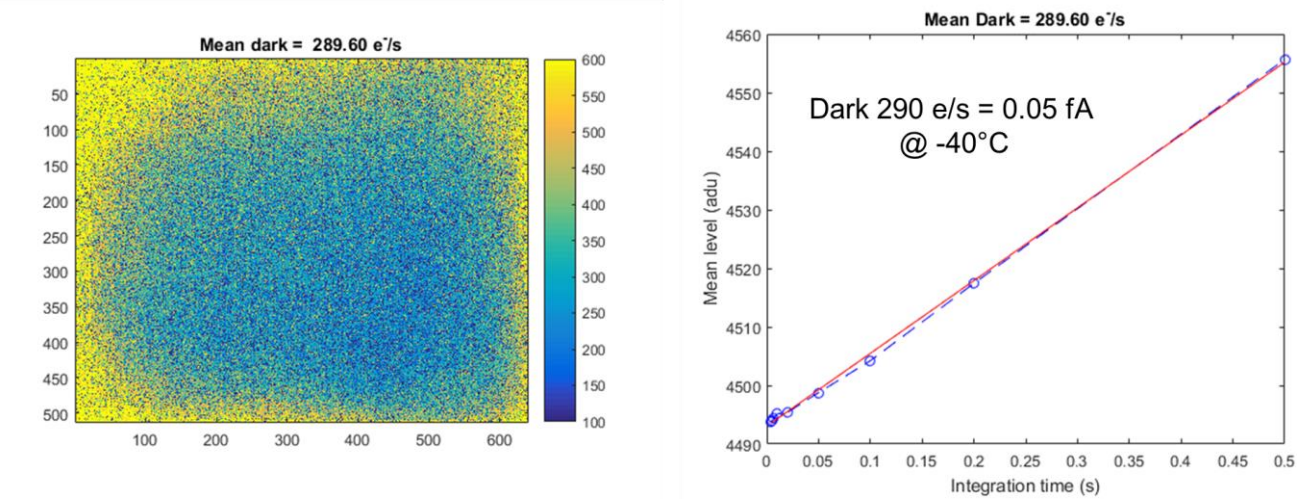

Figure 15: (left) C-RED 2 dark image at -40°C, scale is in e/s; (right) Dark measurement at -40°C by measuring level as a function of the integration time. The camera system gain in 2.33 e/adu. Dark as low as 290 e/s (0.05 fA) is measured here at -40°C.

The Figure 14 and Figure 15 show the dark current measurement from C-RED2. The mean dark current is multiplied by a factor of 2 every 7.5 °C. It also shows that a mean dark current of 290 e/s (0.05 fA) is demonstrated at an operating temperature of -40°C. The value of 290 e/s is a simple average of the dark over all the pixels from the image, deeper cooling does not show an improvement in dark suppression, this might be a ROIC glow. This will be further investigated and optimized out to reduce this ROIC glow like it has been done on the C-RED One camera.

The Figure 16 shows the readout noise of the C-RED 2 camera at 400 FPS in CDS mode (Correlated Double Sampling) with 3µs integration time. A readout noise of 22 e- is achieved at a readout speed of 400 FPS full frame. This type of performance in terms of speed and noise combined has never been achieved so far by the C-RED 2 competitors for a SWIR InGaAs camera.

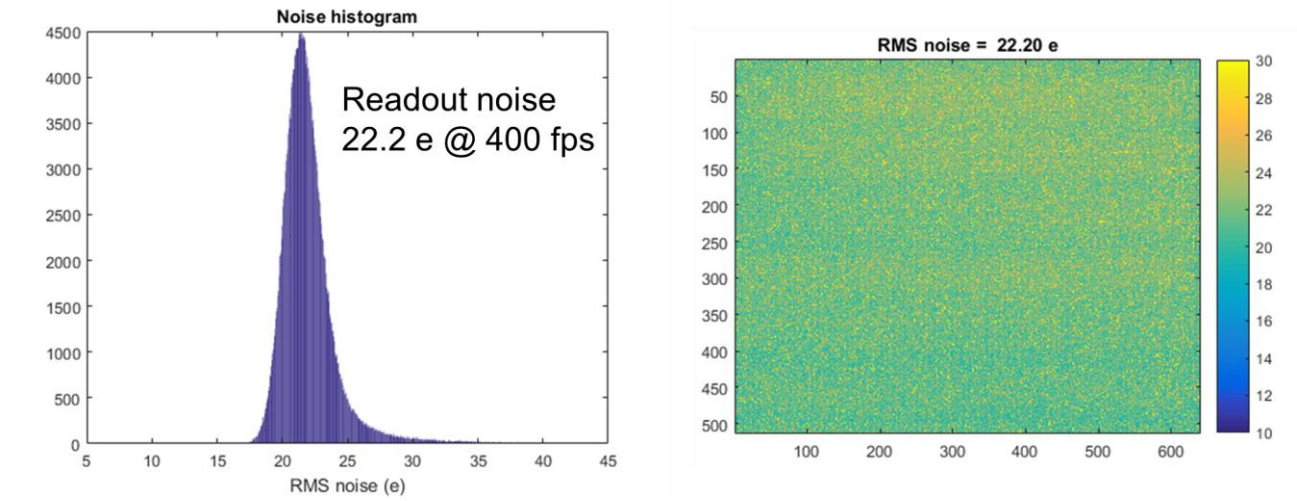

Figure 16: (left) C-RED2 camera readout noise histogram at 400 frames/s and -40°C and 3µs integration time. The mean readout noise is 22.2 e; (right) readout noise image at at 400 frames/s and -40°C.

Non destructive readout

It is possible to perform non destructive reaoduts to decrease the readout noise of the camera. The intensity of each pixel is then computed by linear fitting or fowler sampling. The impact is a frame rate decrease to do the computation over the selected images. There is not much interest to do this with full frame since the dark current will produce a large amount of noise. If this method is used in combination with a windowing, then low RON can be obtained with high frame rate. In the example in Figure 17, the sensor is readout with a 96x80 ROI giving a raw frame rate of 5146FPS. Then 256 NDR samples are used to compute the final image using a linear fit, giving a final frame rate of 20FPS and a RON below 10e-. This is particularly interesting when doing tip-tilt AO correction for example where only a few pixels are needed.

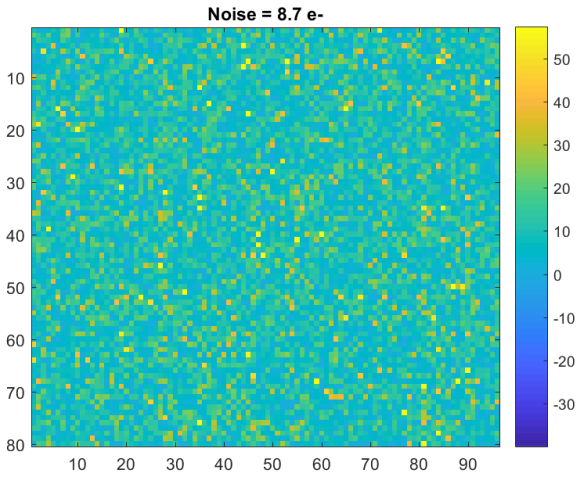

Figure 17: noise map of a cropped 96x80 pixels region with NDR readout (line fitting) giving 8.7e- RON with 256 NDR and a final frame rate of 20 FPS.

4. CONCLUSION

We've demonstrated the ability of CRED One to have comparable or even better performance than visible fast cameras dedicated to AO wavefront sensing like OCAM2 : this camera offers fast frame rate, subelectron noise, low background, wide spectral response over J, H and K bands, and outstanding cosmetics compared to other SWIR cameras. APD technology is now mature enough to be used in scientific applications. An unprecedented noise of 0.4 e was achieved for a SWIR camera at the speed of 3500 FPS . C-RED one permits then a significant advance in short wave infrared imaging and is opening new windows for scientific applications like IR wavefront sensing or fast IR focal plane arrays used in astronomy.

In addition to the C-RED One development, C-RED 2 is InGaAs 640x512 fast camera with unprecedented performances in terms of noise, dark and readout speed based on the SNAKE SWIR detector from Sofradir. A readout noise of 22 e has been obtained at 400 FPS readout speed in CDS mode and 2us integration time. Cooled at -40°C, the C-RED 2 camera is able to achieve a dark current of ~300 e/s (0.05 fA).

C-RED One and C-RED 2 are both SWIR commercial cameras from First Light Imaging fully available and in production now.

REFERENCES

[1] P. Feautrier et al., “OCam with CCD220, the Fastest and Most Sensitive Camera to Date for AO Wavefront Sensing”, Publ. Astron. Soc. Pac. Vol 123 n°901, 263-274 (2011)

[2] J.L. Gach and P. Feautrier, “Electron initiated APDs improve high-speed SWIR imaging”, Laser Focus World vol 51 n°9, 37-39, (2015)

[3] G. finger et al., “Evaluation and optimization of NIR HgCdTe avalanche photodiode arrays for adaptive optics and interferometry”, Proc. SPIE 8453, 84530T (2012).

[4] Feautrier, Philippe, Gach, Jean-Luc, Wizinowich, Peter, "State of the art IR cameras for wavefront sensing using e-APD MCT arrays", AO4ELT4 Conference, 2015. Rouvié, O. Huet, S. Hamard, JP. Truffer, M. Pozzi, J. Decobert, E. Costard, M. Zécri, P. Maillart, Y. Reibel, A. Pécheur “SWIR InGaAs focal plane arrays in France”, SPIE Defense, Security and Sensing, 8704-2 (2013)

[5] Philippe Feautrier, Jean-Luc Gach, Timothée Greffe,, Eric Stadler, Fabien Clop, Stephane Lemarchand, David Boutolleau, “C-RED One and C-RED 2: SWIR advanced cameras using Saphira e-APD and Snake InGaAs detectors”, SPIE 10209, 102090G (2017)

[6] Rouvié, O. Huet, S. Hamard, JP. Truffer, M. Pozzi, J. Decobert, E. Costard, M. Zécri, P. Maillart, Y. Reibel, A. Pécheur “SWIR InGaAs focal plane arrays in France”, SPIE Defense, Security and Sensing, 8704-2 (2013)

[7] J. Coussement, A. Rouvié, EH. Oubensaid, O. Huet, S. Hamard, JP. Truffer, M. Pozzi, P. Maillart, Y. Reibel, E. Costard, D. Billon-Lanfrey “New Developments on InGaAs Focal Plane Array”, SPIE Defense, Security and Sensing, 9070-5 (2014)

[8] Rouvié, J. Coussement, O. Huet, JP. Truffer, M. Pozzi, E.H. Oubensaid, S. Hamard, P. Maillart, E. Costard, “InGaAs Focal Plane Array developments and perspectives”, SPIE Electro-Optical and Infrared Systems, 9249 (2014)

[9] Rouvié, J. Coussement, O. Huet, JP. Truffer, M. Pozzi, E.H. Oubensaid, S. Hamard, V. Chaffraix, E. Costard “InGaAs Focal Plane Array developments and perspectives”, SPIE Defense, Security and Sensing, 9451-4 (2015)